Decoupled Control of a twin hull-based Unmanned Surface Vehicle using a Linear Parameter Varying approach

Echrak Chnib, Olivier Sename, Francesco Ferrante, Eduardo Rodriguez Canales, Juan Cutipa Luque

Decoupled Control of a twin hull-based Unmanned Surface Vehicle using a Linear Parameter Varying approach

Echrak Chnib[1], Olivier Sename[1], Francesco Ferrante[1], Eduardo S. Rodriguez Canales[2], and Juan C. Cutipa Luque[2]

[1] Univ. Grenoble Alpes, CNRS, Grenoble INP
GIPSA-Lab, 38000 Grenoble, France
{echrak.chnib,olivier.sename}@grenoble-inp.fr
francesco.ferrante@gipsa-lab.fr
[2] Electronic Engineering Department
Universidad Nacional de San Agustín de Arequipa
Arequipa, Peru
{erodriguezca,jcutipalu}@unsa.edu.pe

Abstract. This paper presents a decoupled control of a twin hull-based Unmanned Surface Vehicle EDSON-J, using the H_∞ approach for Linear Parameter Varying (LPV) polytopic systems. This method was adapted in order to guarantee robust stability and performance regarding the important non-linearities and the uncertainties on the hydrodynamics parameters. After the presentation of the nonlinear model and the decoupled model of the USV considered for the study, an LPV model was built, regarding the mass of the vehicle as unique varying parameter. Then the methodology of the control law applied is exposed and simulation results are presented. A comparison with the LTI/H_∞ approach will show the interest of the method in terms of performance.

Keywords: Linear parameter varying (LPV), H_∞ robust control, Unmanned surface vehicle (USV), Decoupled control.

1 Introduction

Since two thirds of the Earth's surface is covered by the oceans, the development of water vehicles has been seeing an increasing interest [3]. Over the past decades, several works on Unmanned Maritime Vehicles (UMVs) have been developed comprising unmanned surface vehicles (USVs) and unmanned undersea vehicles (UUVs). As global positioning systems have become more compact, the use of unmanned surface vehicles (USVs), also known as autonomous surface crafts (ASCs), in performing complex tasks has become more and more popular [9]. Applications in which USVs are used include mine counter measures (MCM), inspections for inshore environmental monitoring [10]. An overview on the research and applications of USVs is presented in [7].

Due to cross-coupled dynamics and the presence of hydro-dynamic forces, the design of efficient control systems for UMVs is generally challenging. In [13], a nonlinear gain-scheduling control was proposed to control the INFANTE AUV. A diving-control

design, based on Lyapunov theory and backstepping techniques, is proposed to control an AUV in [5]. In [2], a robust H_∞ control approach, based on a two-degrees-of-freedom controller, was developed for the control of AUV. Recently, a nonlinear control scheme based on the energy-shaping (ES) principle and state error port-controlled Hamiltonian (PCH) systems has been proposed in [8]. The design of robust adaptive steering controllers was proposed in [15] to deal with the control of USVs in the presence of uncertainties, unknown control direction, and input saturation.

For systems with predominant nonlinear behaviors and large parameter uncertainties, the use of robust control techniques, such as H_∞ control, may not be sufficient to achieve good performance over the full range of parameter variation. In this setting, a possible approach to guarantee robustness and performance consists of relying on Linear Parameter Varying (LPV) polytopic models and H_∞ control; see, e.g., [11]. In the last years, the use of LPV controllers has shown to be effective in the control of autonomous surface craft. In [6], the authors presented an LPV controller with adaptive parameter estimation and adaptation capabilities. More recently, in [12] an LPV robust control system for a twin hull-based unmanned surface vehicle, named EDSON-J, was developed to account for mass variation considering a set of controllers generated by using the so-called grid-based approach.

In this paper, we aim to extend the design of LPV controllers for EDSON-J model by considering a decoupled control approach. In particular, due to the inherent complexity in embedding the LPV controller proposed [12] on a low-cost platform, the major contribution of this paper consists of designing two independent controllers for both lateral motion and longitudinal motion guaranteeing performance and robustness. This leads to controllers that can be easily implemented in low-cost embedded systems, thereby making our results more appealing in practice.

The paper is organised as follows. Section 2 presents the EDSON-J architecture. The decoupled model into surge-yaw of the USV is considered in Section 3. Section 4 presents the proposed H_∞/LTI surge-yaw decoupled control. The LPV surge-yaw decoupled control is developed in Section 5. Section 6 discusses the obtained simulation results followed by conclusions in section 7.

2 EDSON-J architecture

The EDSON-J is a twin hull-based Unmanned Surface Vehicle that has been developed at the University of San Agustin de Arequipa, Peru in 2019. This autonomous vessel is designed to perform inspection and monitoring tasks in the Pacific sea coastal and lagoons of Arequipa. Table 1 summarizes the main mechanical specifications of this USV. The vehicle design consists of two slender bodies propelled by two electric motors in differential mode n_d and common mode n_c. The EDSON-J's operating speed is 1.5 m/s with a maximum speed of 2.5 m/s. The vessel power supply is provided by two 100 Ah AGM batteries. The navigation system of the USV is based on a dual GNSS/INS system in order to ensure the position accuracy, velocity and acceleration measures.The communication system is provided by RF transceivers, with a range of 96.56 km in the 900 MHz spectrum. The control architecture of the vehicle is consisting of an embed-

Parameter	Value
Length	3.00 m
Breadth	1.60 m
Mass	250 kg
Payload	100 kg
Hull breadth	0.30 m
Draft	0.20 m
Moment of inertia	201.1 kg/m^2
Location of mass center	0.11 m
Electric motor power (each)	600 W

Table 1: EDSON-J USV dimensions

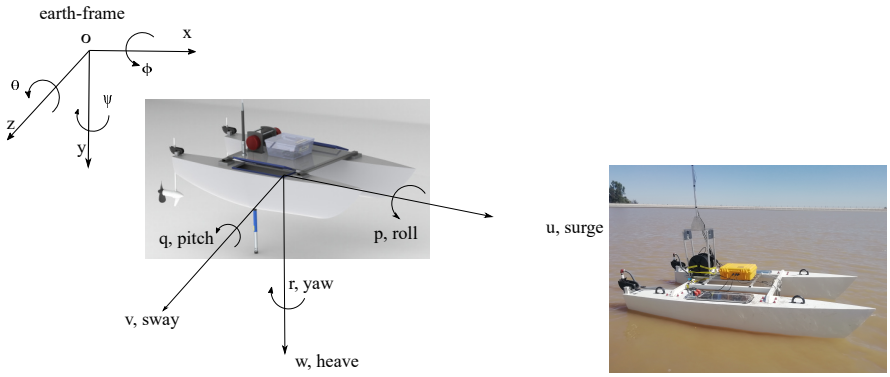

Fig. 1: coordinate frames of the EDSON-J [12]

ded computing board with an operative robotic system (ROS) running on GNU/Linux for the implementation of the control algorithms.

2.1 Nonlinear model of the EDSON-J

According to the nomenclature given in [4], the mathematical model of the surface vehicle has been developed by considering the interaction between the rigid body dynamics (hull structure) and hydrodynamics forces interaction (the fluid). The Fig1 presents the earth-frame and the rigid body-frame fixed at the centroid of the USV. The inertial frame is represented by the position vector $\eta = \begin{bmatrix} x & y & \psi \end{bmatrix}^T$ where x is the surge position, y is the sway position and ψ is the yaw position. The body-frame is represented by the velocity vector $\nu = \begin{bmatrix} u & v & r \end{bmatrix}^T$ where u is the linear velocity of the surge, v is the linear velocity of the sway and r is the angular velocity of the yaw. Then the nonlinear model of the EDSON-J can be represented by the kinematic and dynamic equations, respectively (1) and (2):

$$\dot{\eta} = J(\eta)\nu \tag{1}$$

$$M\dot{\nu} + C(\nu)\nu + D(\nu)\nu = \tau \tag{2}$$

where $\dot{\eta}$ stands for the derivative of the position vector η and $J(\eta)v$ the coordinate transformation matrix from the earth-frame to the body-frame defined as:

$$J(\eta) = \begin{bmatrix} \cos(\psi) & -\sin(\psi) & 0 \\ \sin(\psi) & \cos(\psi) & 0 \\ 0 & 0 & 1 \end{bmatrix} \tag{3}$$

$\tau := \begin{bmatrix} X & Y & N \end{bmatrix}^T$ is the vector of the generalized input forces originated by the propeller actuators. X is the force in surge direction, Y is the force in sway direction and N is the moment in yaw direction. The dynamic equation is defined by its inertia matrix M, the C matrix containing Coriolis and centrifugal forces, and the damping matrix D. These matrices are expressed as follows:

$$M = \begin{bmatrix} m - X_{\dot{u}} & 0 & 0 \\ 0 & m - Y_{\dot{v}} & mx_g - Y_{\dot{r}} \\ 0 & mx_g - N_{\dot{v}} & I_z - N_{\dot{r}} \end{bmatrix} \tag{4}$$

$$C = \begin{bmatrix} 0 & -mr & -mx_g r + Y_{\dot{v}} v + Y_{\dot{r}} r \\ mr & 0 & -X_{\dot{u}} u \\ mx_g r - Y_{\dot{v}} v - Y_{\dot{r}} r & X_{\dot{u}} u & 0 \end{bmatrix} \tag{5}$$

$$D = \begin{bmatrix} X_u + X_{|u|u}\,|u| & 0 & 0 \\ 0 & Y_v + Y_{|v|v}\,|v| & 0 \\ 0 & 0 & N_r + N_{|r|r}\,|r| \end{bmatrix} \tag{6}$$

where m is the USV mass, x_g the position of center of mass and I_z the moment of inertia around the z axis, $X_{\dot{u}}$, $Y_{\dot{v}}$, $Y_{\dot{r}}$, $N_{\dot{v}}$ and $N_{\dot{r}}$ are the hydrodynamic terms related to added masses. The terms X_u, Y and N_r represent the linear drag coefficients, while $X_{|u|u}$, $Y_{|v|v}$ and $N_{|r|r}$ are the quadratic drag coefficients [12].

2.2 Hydrodynamic coefficients

The vehicle parameters can be obtained through either empirical relations or numerical/computational methods using the slender-body theory and the rigid body dynamics. The parameters of the USV nonlinear model are reported in Table 2. More details about the hydrodynamic coefficients can be found in [12].

3 Decoupled models of the EDSON-J

This section presents the decoupled model of the EDSON-J into two subsystems: the surge and the sway/yaw. From the nonlinear model of the EDSON-J expressed by (1) and (2), we derive a linearized model of the following form:

$$G : \begin{cases} \dot{x} = Ax + B\chi \\ y = Cx + D\chi \end{cases} \tag{7}$$

$x = \begin{bmatrix} u & v & r \end{bmatrix}^T$ is the state vector, $\chi = \begin{bmatrix} n_c & n_d \end{bmatrix}^T$ is the control input vector, and $y = \begin{bmatrix} u & r \end{bmatrix}^T$ is the output vector. Matrices A, B, C and D are obtained by Jacobian linearization around the cruise speed u_0=2 m/s and a rotational speed n_0=14 rps.

Parameter	Value	Unit	Parameter	Value	Unit
$X_{\dot{u}}$	-2.471	Kg	X_u	-0.2912	Kg/s
X_{uu}	-27,626	Kg/m	X_{un_c}	-3.682	Kg
X_{rn_d}	2.762	Kg	$X_{n_cn_c}$	1.052	Kg/m^2
$X_{n_dn_d}$	1.052	Kg/m^2	$Y_{\dot{v}}$	-247.065	Kg
$Y_{\dot{r}}$	-370.597	Kg.m/rad	Y_v	-164.71	Kg/s
Y_{vv}	-38.928	Kg/m	Y_{vn_c}	-0.359	Kg
Y_{rn_c}	-0.538	Kg.m	$N_{\dot{r}}$	-748.310	Kg.m^2/rad
$N_{\dot{v}}$	-370.597	Kg.m	N_r	-988.260	Kg.m^2/rad.s^2
N_{rr}	-262.791	Kg.m^2.rad^2	N_{un_d}	2.762	Kg.m
N_{rn_c}	-2.855	Kg.m^2	$N_{n_Cn_d}$	-1.578	Kg.m^2
N_{vn_c}	-0.538	Kg.m			

Table 2: EDSON-J USV parameters

3.1 Surge and Sway/Yaw LTI models

Surge LTI model The surge system corresponds to the dynamics of the state u in (7), with control input n_c and measured output $y_s = u$. A state space representation of this system is given next, with $x_s = u$:

$$S : \begin{cases} \dot{x}_s = A_s x_s + B_s n_c \\ y_s = C_s x_s + D_s n_c \end{cases} \tag{8}$$

$$A_s = \frac{-X_u - X_{un_c} n_0 - 2X_{uu} u_0}{X_{\dot{u}} - m}, \;\; B_s = \frac{-2X_{n_c n_c} n_0 - X_{un_c} u_0}{X_{\dot{u}} - m} \tag{9}$$

$$C_s = 1, \;\; D_s = 0 \tag{10}$$

Sway/Yaw LTI model The sway/Yaw system corresponds to the dynamics of the state vector $x_{sy} = \begin{bmatrix} v & r \end{bmatrix}^T$ in (7), the control input n_d and the measured output vector $y_{sy} = r$. It can be represented by the following state space equations:

$$SY : \begin{cases} \dot{x}_{sy} = A_{sy} x_{sy} + B_{sy} n_d \\ y_{sy} = C_{sy} x_{sy} + D_{sy} n_c \end{cases} \tag{11}$$

3.2 Surge and Sway/Yaw LPV models

The above models are LTI models if the mass m is known and fixed. As opposed, when the mass takes value in $[m_{min}, m_{max}]$, those models can be represented as LPV systems; see, e.g., [12], wherein a similar approach is pursued.

Surge LPV model As seen in (9), the matrices A_s and B_s depend on m in a nonlinear fashion. To obtain a control-oriented LPV model we can set

$$\rho_s = \frac{1}{X_{\dot{u}} - m} \tag{12}$$

which enable to obtain the following LPV model for the surge dynamics:

$$S(\rho_s):\begin{cases}\dot{x}_s = A_s(\rho_s)x_s + B_s(\rho_s)n_c \\ y_s = C_s x_s + D_s n_c\end{cases} \tag{13}$$

note that A_s and B_s are affine in ρ_s. Such a model can be easily written in a polytopic form, thereby allowing to simplify the design of a controller as detailed next.

Sway/Yaw LPV model The matrices A_{sy} and B_{sy} also depend on m in a nonlinear fashion. However, since the mass appears both in the numerator and denominator of the entries of the matrices A_{sy} and B_{sy}, to get an LPV representation, one needs to introduce two parameters. In particular, we define

$$\rho_{sy}^1 := \frac{1}{(I_z Y_{\dot{v}} + m^2 x_g^2 - N_{\dot{r}} Y_{\dot{v}} - m I_z + m N_{\dot{r}} + Y_{\dot{r}}^2 - 2m x_g Y_{\dot{r}})} \tag{14}$$

$$\rho_{sy}^2 := \frac{m}{(I_z Y_{\dot{v}} + m^2 x_g^2 - N_{\dot{r}} Y_{\dot{v}} - m I_z + m N_{\dot{r}} + Y_{\dot{r}}^2 - 2m x_g Y_{\dot{r}})} \tag{15}$$

Following this approach, the Sway/Yaw LPV model writes:

$$SY(\rho_{sy}):\begin{cases}\dot{x}_{sy} = A_{sy}(\rho_{sy})x_{sy} + B_{sy}(\rho_{sy})n_d \\ y_{sy} = C_{sy}x_{sy} + D_{sy}n_d\end{cases} \tag{16}$$

where A_{sy} and B_{sy} are affine in $\rho_{sy} \in \mathbb{R}^2$.

4 H_∞/LTI surge-yaw decoupled control

The H_∞ control problem consists in finding a control that aims at minimizing the H_∞ norm of the closed-loop system [14]. Defining w the exogenous input vector, and e the controlled output vector, the H_∞ suboptimal control problem is, given γ a predefined attenuation level, to design a controller that internally stabilizes the closed-loop system and ensures:

$$\|T_{ew}\|_\infty \leq \gamma \tag{17}$$

where T_{ew} is the closed-loop transfer matrix from w to e. The minimal value γ_{opt} is then approached by a bisection algorithm. The considered H_∞ control scheme for the two problems is chosen as in Fig. 2.
Such an H_∞ control problem can be efficiently solved by relying either on Riccati equations or linear matrix inequalities. This leads to the design of the control law u_K that solves the suboptimal problem (17) (or optimal when γ is minimized); (see [14]).

4.1 Surge–Yaw decoupled H_∞ control

In this section, we present the structure and weighting functions selected for each decoupled subsystem.

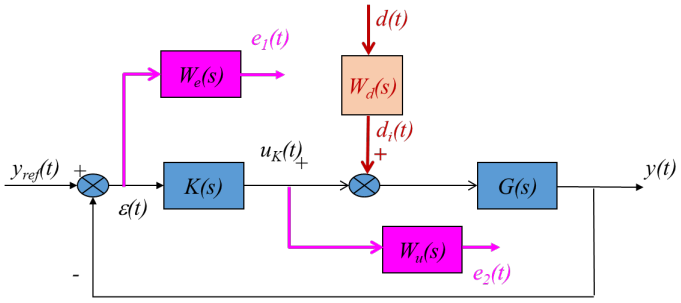

Fig. 2: Structure chosen for the Surge/Yaw controller design

Performance specifications for the Surge-Yaw The weights on the sensitivity function W_{e_u} in surge velocity u and W_{e_r} yaw rate r are expressed by:

$$\frac{1}{W_{e_u}} = \frac{s + \omega_{bu}\varepsilon_{1u}}{\frac{s}{M_{eu}} + \omega_{bu}} \quad , \quad \frac{1}{W_{e_r}} = \frac{s + \omega_{br}\varepsilon_{1r}}{\frac{s}{M_{er}} + \omega_{br}} \tag{18}$$

- For the surge :
  M_{eu}= 2 to ensure good robustness margin, ε_{1u}= 0.001 to ensure a tracking error less then 1%,ω_{bu}= 0.46 to ensure a fast closed-loop tracking response and rejection of disturbances.
- For the yaw :
  M_{er} =2, ε_{1r} = 0.001 and ω_{br}= 0.5.

The weights on the controller sensitivity function W_{u_u} in surge velocity u and W_{u_r} yaw rate r are expressed by:

$$\frac{1}{W_{u_u}} = \frac{\varepsilon_{2u}s + \omega_{bc_u}}{s + \frac{\omega_{bc_u}}{M_{uu}}} \quad , \quad \frac{1}{W_{u_r}} = \frac{\varepsilon_{2r}s + \omega_{bc_r}}{s + \frac{\omega_{bc_r}}{M_{ur}}} \tag{19}$$

- For the surge:
  M_{uu}=16 in order to account for actuator limitations, ω_{bcu}=250 and $\varepsilon_{2u} = 0.001$
- For the yaw:
  M_{ur}=80 ω_{bcr}=250 and $\varepsilon_{2r} = 0.001$

Finally the weighting function W_d is set to 0.2 for the surge motion, this enables to handle the coupling with the surge dynamics, while it is set to 0 for the yaw control. Indeed, the yaw dynamics are practically decoupled from the surge.

Solving the above H_∞ control problems leads to $\gamma_{min} = 0.77$ for the surge motion, and $\gamma_{min} = 0.88$ for the yaw motion. This allows to conclude that both LTI controllers satisfy the performance requirements in the nominal case. Moreover, it may be shown that, using a μ-analysis, both controllers keep stability considering some mass uncertainty, mainly due to pay load variations, i.e. when $m \in [250, 400]$. However they do not achieve robust performance, which emphasizes the need for an LPV controller to ensure the satisfaction of the performance requirements for large mass variations, in particular for the yaw controller. This is the objective of the following section.

5 LPV surge-yaw decoupled control of the EDSON-J

In this section, we develop LPV mass-dependent controllers for the surge and yaw dynamics. This is enabled by the use of the LPV models presented in Section 3. The formulation of the LPV control problem follows closely the one presented for the LTI case, using the same weighting functions for performance requirements.

5.1 LPV control problem

The considered LPV control problem for the surge and yaw dynamics are a direct extension of the ones proposed for the LTI control problems, yet applied on the LPV models. The control scheme is as in Fig 3.

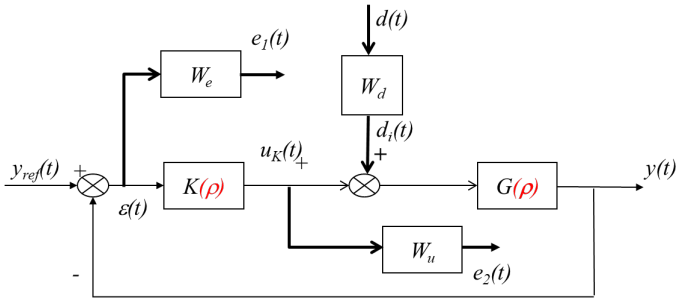

Fig. 3: LPV Surge/Yaw control design scheme.

As mentioned earlier, it is worth noting that the weighting functions are the same for the LPV control problem than for the LTI one. This allows a fair comparison between both methodologies.

As explained in Section 3, the LPV surge and yaw models are affine with respect to the chosen parameters vector. This means that we can apply the polytopic approach to design both LPV controllers. This is the objective of the next section.

5.2 LPV polytopic controller

The LPV controller is designed using the polytopic approach presented in [1]. The applicability of the so-called polytopic method is restricted to LPV systems whose matrices depend in an affine fashion on the vector of parameters. More precisely

$$A(\rho) = A_0 + \sum_{i=1}^{n_p} A_i \rho_i \tag{20}$$

In this case, the LPV system can be written as a polytopic system with 2^{n_p} vertices, where n_p is the number of the varying parameters.

In the LPV/H_∞ framework, the control synthesis problem is addressed off-line by solving a set of LMIs at each vertex of the polytope using convex optimization. The parameter dependent LPV output-feedback controller is designed to guarantee the quadratic stability of the closed-loop system, together with a minimal $\mathscr{L}_2$-induced gain from the external input w to the controlled output vector e, i.e., to ensure that $||T_{ew}||_{\mathscr{L}_2-\mathscr{L}_2} < \gamma$ (where γ is to be minimized). The solution of the problem are the vertex LTI controllers, $K_i = \begin{bmatrix} A_i & B_i \\ C_i & D_i \end{bmatrix}$, where $1 \leq i \leq 2^{n_p}$. The polytopic LPV controller $K(\rho)$ is computed on-line as the convex combination of the vertex controllers K_i.

$$K(\rho) = \sum_{i=1}^{2^{n_p}} a_i(\rho) K_i, \text{ with } \sum_{i=1}^{2^{n_p}} a_i(\rho) = 1 \tag{21}$$

$$a_i(\rho) = \frac{\prod_{j=1}^{n_p} |\rho_j - C^c(\omega_i)_j|}{\prod_{j=1}^{n_p} (\overline{\rho_j} - \underline{\rho_j})} > 0, \quad \text{with } C^c(\omega_i)_j = \begin{cases} \overline{\rho_j} & if\ \omega_i = \underline{\rho_j} \\ \underline{\rho_j} & otherwise \end{cases} \tag{22}$$

$\overline{\rho_j}$, $\underline{\rho_j}$ are the upper and lower bounds of the j^{th} element of the varying parameter vector respectively and ρ_j is its instantaneous measured value.

5.3 LPV design for surge and yaw motion

First let us recall the the LPV surge model has one parameter while the yaw one has 2 parameters. Considering the polytopic approach, the LPV surge control problem includes a polytope of 2 vertices, while the LPV yaw control problem handles a polytope of 4 vertices, as can be seen later in the frequency-domain plots of the sensitivity functions.

Solving the LPV/H_∞ control problems leads to find the minimal attenuation level γ for both problems. Table 3 summarizes these results for the LPV controllers, compared with the solution of the corresponding LTI problems.

	γ_{min} LTI case	γ_{min} LPV case
Surge control	0.77	0.91
Yaw control	0.88	1.22

Table 3: H_∞ performances of the LTI and LPV closed-loop systems

This result means that, solving the LPV yaw control problem induces some conservatism. This is due to the problem solution using a single Lyapunov function for the 4 vertices of the polytope. This problem can be overcome as in [12] using the gridding approach, but the latter generates a large set of controllers to be implemented, which is much more complicated to embed in a real system.

6 Simulation results

In this section time-domain simulation have been performed using the complete non-linear model of the EDSON-J USV presented in [12]. Two scenario are presented to show the impact of the mass variations on the performances on both LTI and LPV control strategies.

6.1 Initial Evaluation

This first test is a basic step-response of the surge and yaw motion, here performed for the nominal ($m = 250kg$) and worst ($m = 400kg$) mass parameter value. As can be seen

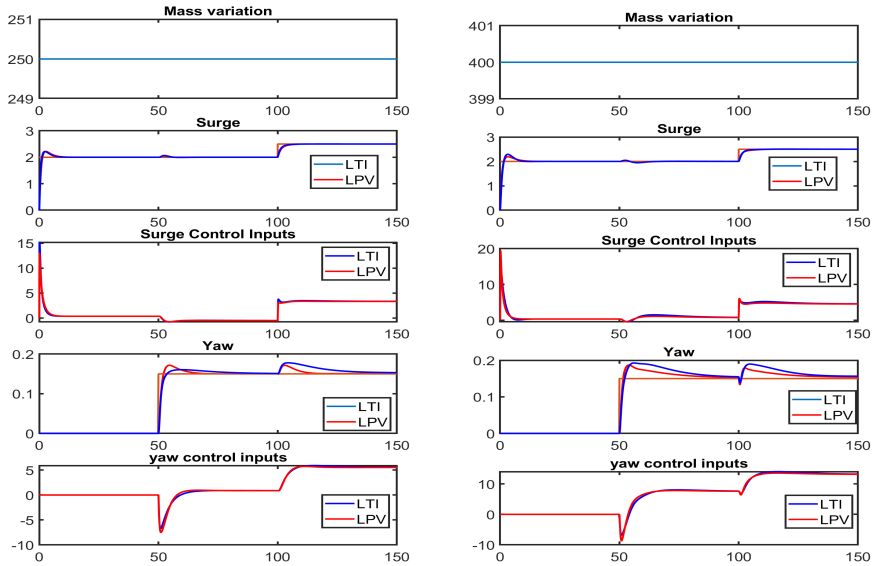

Fig. 4: Steps responses of LTI vs LPV surge/yaw controllers for the nominal (left) and maximal (right) mass value

on Fig 4, the surge motion is few affected by the difference of mass and performs well for the LTI and LPV control. However, while the yaw motion is few affected in the LPV case, it is deteriorated a lot in the LTI case for the maximal mass. This is coherent with the Robust Performance analysis carried out in section 3 where we showed that the LTI yaw controller is not robust in performance.

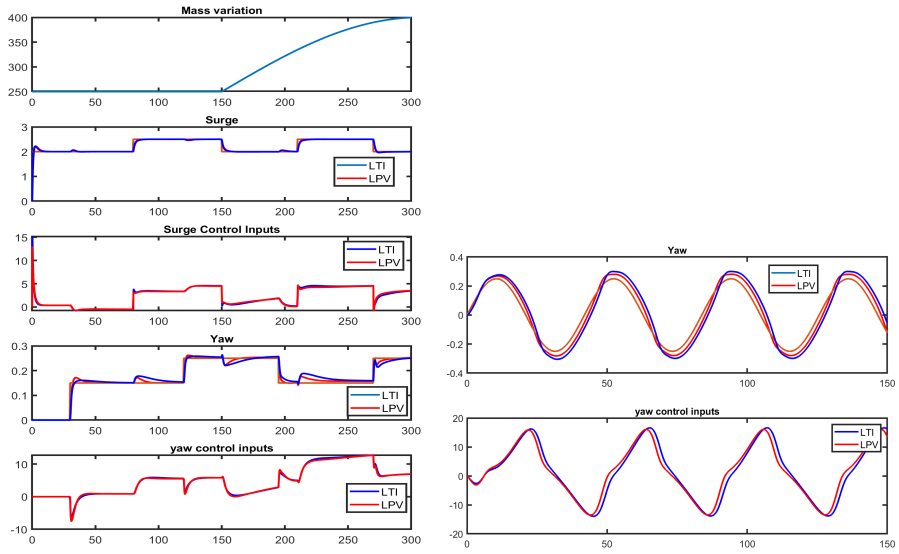

Fig. 5: LTI vs LPV decoupled control : scenario 1 (left) and scenario 2 (right)

6.2 Scenario 1

In this scenario, the surge and yaw and motion are following a series of step references. This allows to evaluate the performances of the controllers, in particular due to the coupling between longitudinal and lateral motions. As we can see on Fig 5, the surge variable is controlled efficiently by both LTI and LPV controllers, even when the mass is varying.
However, concerning the yaw motion, it can be seen then the LTI controller is more affected by the change of mass than the LPV controller. Indeed if we compute the Root Mean Square error between the yaw and its reference, from $t = 150sec$ (when the mass starts to change), then we get

$$RMSE(r - r_{ref})_{LPV} = 0.0130 \quad RMSE(r - r_{ref})_{LTI} = 0.0172$$

So the LPV method improves the yaw performance by 24.4% in this scenario.

6.3 Scenario 2

In this scenario the mass is assumed to be constant for the worst case ($m = 400kg$), the speed motion is kept constant at $u_0 = 2m/s$ and the yaw is following a sinusoidal reference between -0.25 and $0.25rad/s$. In this case, if we compute the Root Mean Square error between the yaw and its reference then we get

$$RMSE(r - r_{ref})_{LPV} = 0.0389 \quad RMSE(r - r_{ref})_{LTI} = 0.0659$$

So the LPV method improves the yaw performance by 40.97% in this scenario.

7 Conclusion

This paper studied the problem of robust control of the Unmanned Surface Vehicle EDSON-J. LPV mass-dependent controllers were designed in the framework of H_∞ control to fulfill performance requirements over a wide range of mass variations. The approach is deployed on a simplified model in which longitudinal and lateral dynamics are assumed to be decoupled.

Numerical simulations performed on the actual nonlinear system showed the effectiveness of the LPV control to achieve the desired performance despite the coupling between longitudinal and lateral dynamics. Comparisons with LTI controllers showed that the proposed LPV decoupled control yields better performance.

Future works may concern the design of LPV controllers to account for other parameter variations (as the hydrodynamic ones), the comparison with the global approach in [12], and the experimental validation on the real USV.

References

1. P. Apkarian and P. Gahinet. A convex characterization of gain-scheduled $\mathscr{H}_\infty$ controllers. *IEEE Trans. Autom. Contr.*, 40(5):853–864, 1995.
2. J. C. Cutipa-Luque, D. Donha, J. L. D. Dantas, L. M. de Oliveira, and E. A. de Barros. Robust control of an underactuated auv. *IFAC Proceedings Volumes*, 45(27):138–143, 2012.
3. Y. Dinstein and A. W. Dahl. Section iv: Unmanned maritime systems. In *Oslo Manual on Select Topics of the Law of Armed Conflict*, pages 43–53. Springer, 2020.
4. T. I. Fossen. *Handbook of marine craft hydrodynamics and motion control*. John Wiley & Sons, 2011.
5. L. Lapierre. Robust diving control of an auv. *Ocean Engineering*, 36(1):92–104, 2009.
6. Z. Liu, C. Yuan, and Y. Zhang. Linear parameter varying adaptive control of an unmanned surface vehicle. *IFAC-PapersOnLine*, 48(16):140–145, 2015.
7. Z. Liu, Y. Zhang, X. Yu, and C. Yuan. Unmanned surface vehicles: An overview of developments and challenges. *Annual Reviews in Control*, 41:71–93, 2016.
8. C. Lv, H. Yu, Z. Hua, L. Li, and J. Chi. Speed and heading control of an unmanned surface vehicle based on state error pch principle. *Mathematical Problems in Engineering*, 2018, 2018.
9. J. E. Manley. Unmanned surface vehicles, 15 years of development. In *OCEANS 2008*, pages 1–4, 2008.
10. J. E. Manley. Unmanned maritime vehicles, 20 years of commercial and technical evolution. In *OCEANS 2016 MTS/IEEE Monterey*, pages 1–6, 2016.
11. E. Roche, O. Sename, and D. Simon. Lpv/h_∞ control of an autonomous underwater vehicle (auv). In *Proceedings of the European control conference*, pages 3160–3165, 2009.
12. E. S Rodriguez-Canales and J. C. Cutipa-Luque. Lpv/h_∞ control of a twin hull-based unmanned surface vehicle. *Journal of Control, Automation and Electrical Systems*, 32(2):245–255, 2021.
13. C. Silvestre and A. Pascoal. Control of the infante auv using gain scheduled static output feedback. *Control Engineering Practice*, 12(12):1501–1509, 2004.
14. S. Skogestad and I. Postlethwaite. *Multivariable Feedback Control. Analysis and Design*. John Wiley and Sons, Chichester, 2005.
15. S. Wang, M. Fu, and Y. Wang. Robust adaptive steering control for unmanned surface vehicle with unknown control direction and input saturation. *International Journal of Adaptive Control and Signal Processing*, 33(7):1212–1224, 2019.